ACS OMEGA

http://pubs.acs.org/journal/acsodf

Article

Synthesis of a Dual-Functional Nanofertilizer by Embedding ZnO and CuO Nanoparticles on an Alginate-Based Hydrogel

S. Amanda Ekanayake and Pahan I. Godakumbura*

Cite This: *ACS Omega* 2021, 6, 26262–26272

Read Online

ACCESS | Metrics & More | Article Recommendations

ABSTRACT: Recent scientific breakthroughs in the field of agriculture have led to the abundant usage of nanoparticles in agrochemicals to maintain proper nutrient uptake in plants. Since less attention has been given to the supply of vital micronutrients to crop plants, the objective of this study was to develop a nanofertilizer capable of releasing micronutrients while nourishing its surrounding soil. As the initial nanonutrients, Zn and Cu were used in their metal oxide forms, which promote seed germination. Alginic acid was used as the agent responsible for soil conditioning. To form the fertilizing complex, nanoparticles were reacted with sodium alginate, which resulted in a hydrogel where alginate chains were cross-linked with Zn(II) and Cu(II) and excess metal oxide nanoparticles were distributed on the hydrogel. Spectroscopic characterization of the nanofertilizer confirmed that alginate chains were cross-linked by Zn(II) and Cu(II), while morphological analysis by scanning electron microscopy (SEM) showed that ZnO and CuO nanoparticles were embedded on the alginate matrix. The release behavior of cations in soil and water environments, experimented using the tea bag method, revealed that the cationic release was slowly increasing with time. Micronutrient uptake by plants was studied by conducting leaf analyses in tomato plants for 30 consecutive days. To experiment the release behavior of micronutrients in the presence of compost, the nanofertilizer was added with predetermined amounts of compost to tomato plants. Flame atomic absorption spectroscopy (FAAS) results indicated that in the fertilizer-applied plants, Cu concentrations showed a steady increase with time while Zn concentrations remained undetected.

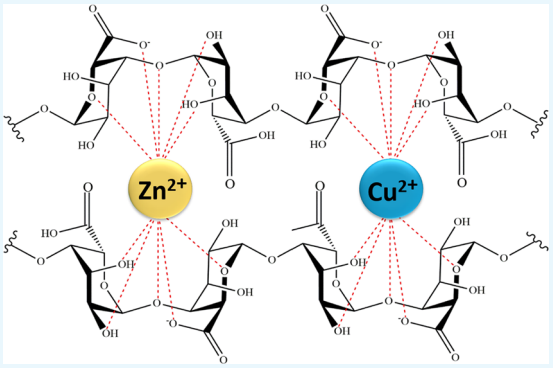

INTRODUCTION

Although plant micronutrients are required in relatively small quantities for crop growth, they are highly important for plant metabolic reactions including photosynthesis, nitrogen fixation, cation neutralization, and amino acid production. Lack of adequate amounts of micronutrients causes unfavorable effects on plants including stunted growth, chlorosis and deformation of plant leaves, lower yields, and reduced quality of plant products. Due to intense agricultural practices that have been used in the last few decades, natural micronutrient pools in soil have been exhausted, highlighting the importance of developing micronutrient fertilizers. One of the early methods used to provide micronutrients to plants was to add them to NPK fertilizers at lower rates. But when these combined fertilizers are added to the soil, these micronutrients have the tendency to form chemical precipitates with different anions present in the soil or interact with clay colloids or wash off to deeper layers of soil, making them unavailable for plant uptake during its growth.[1]

Micronutrient fertilizers that have been developed so far fall into four major categories: fertilizers with lower solubility, fertilizers with an external coating, fertilizers based on biological materials, and nanofertilizers.[1] Slow-release fertilizers (SRFs) and controlled-release fertilizers (CRFs) fall into the category of fertilizers with lower solubility since micronutrients contained within are released only after breaking bonds with its surrounding compounds, e.g., metaphosphates and phosphate glasses. Improved CRFs have led to the formation of fertilizers with external coatings, where the granules contained in the fertilizer are coated, usually with a synthetic or natural polymer (such as sulfur, polydopamine, gelatin) so that the micronutrients contained in the granules diffuse outside at a slower rate. As an alternative to nonbiodegradable CRFs, fertilizers based on biological materials were developed, where the ability of various biological compounds such as alginate or chitosan to bind with micronutrient cations through various functional groups, was utilized.[1] As the name implies, a nanofertilizer is formed by making use of particles with dimensions in the order

Received: June 22, 2021
Accepted: September 13, 2021
Published: September 28, 2021

of 100 nm to form a variety of agrochemicals to maintain proper nutrient distribution and uptake in plants as well as for efficient weed and pest control. These agrochemicals include nanofertilizers, nanoherbicides and nanopesticides, nanoagrochemicals, nanobiosensors, and nano-based handling of agricultural effluents.[2] A nanofertilizer can be considered as a synthesized or a modified form of traditional fertilizer, synthesized using various chemical and mechanical methods with the help of nanotechnology. These nanofertilizers are mainly used to improve the quality of agricultural products and to improve crop production.[2,3] In nanofertilizers, nutrients can be encapsulated by nanomaterials, covered with a thin film or delivered as nanoparticles (NP).[4] Such a nanofertilizer is capable of providing nutrients to plants, nourishing the soil to an organic state, enhancing the overall crop yield and biomass growth of crop plants.[1] Due to the smaller particle size, these nanonutrient particle-based nanofertilizers have a high surface area, which provides more sites to facilitate metabolic reactions within the plant, resulting in higher rates of photosynthesis. Since the particle size of nanonutrients is lesser than that of the pore size of plant root cells, when the nanofertilizer is applied to soil, it allows increased penetration of the nanoparticles to root cells, increasing the nutrient absorption and uptake by the plant root system.

The newest trend in the field of agricultural fertilizers is the development of superabsorbent hydrogels (SAHs) due to the ability to retain water and regulate nutrients release in one material. As discussed above, SRFs and CRFs release their nutrients at a slower rate and this is achieved by the use of a polymeric coating through which the encapsulated nutrients have to diffuse to be released. Although there have been many instances where these SAHs have been combined with SRFs and CRFs, most of these combinations make use of nonbiodegradable synthetic polymers such as polyacrylic acid and polyacrylamide, in the part containing the SRFs and CRFs.[5] Hence, the use of natural polymers in the formation of fertilizers has become a major concern to develop biodegradable novel fertilizer formulations with abundant and low-cost starting materials. Ramli et al. give a detailed description on how different types of SAHs and SRFs have been synthesized with the use of natural polysaccharides, and these include the ones synthesized using chitosan, cellulose, gellan gum, alginates, lignin, and combinations of these biopolymers.[5]

In the development of the micronutrient nanofertilizer, this study was focused on the use of alginic acid, a naturally occurring polysaccharide distributed widely in the cell walls of brown algae. Alginic acid was specifically chosen because of its ability to act both as a plant conditioner and a soil conditioner. Considering its structure, alginic acid is a macromolecule composed of α-L-guluronic acid and β-D-mannuronic acid. The presence of secondary hydroxyl groups at C-2 and C-3 positions and a carboxyl group at C-6 position makes alginic acid hydrophilic and modifiable under various reaction conditions.[6] This feature of this biopolymer was employed in developing the intended nanofertilizer in this study. When alginate chains are cross-linked with divalent and trivalent cations, the resulting hydrogel helps to retain water in soil by forming a crumb structure and this creates favorable conditions for the growth of plant roots.[7] The mechanism related to the alginate hydrogel formation via divalent and trivalent cation cross-linking, enabling them to absorb significant amounts of water without undergoing any structural deformation, has been extensively studied in many instances.[6,8−12] The presence of various functional groups including hydroxyl, carboxyl, and carbonyl groups in the structure of alginic acid enables cross-linking which in turn paves the way to act as an SAH.

There have been numerous studies conducted on the use of alginic acid to form SRFs and CRFs, but most of these fertilizers have made use of synthetic polymers and coatings to enhance the slow-releasing behavior of the nutrients. Sodium alginate-*g*-poly(acrylic acid-*co*-acrylamide)/clinoptilolite (NaAlg-*g*-poly(AAc-*co*-AAm)/clin) and MMt-based NaAlg-*g*-poly(AAc-*co*-AAm) are two examples of hydrogel nanocomposites that have been used as combined synthetic−natural SRFs made using synthetic polymers and inorganic materials.[5,11,12] As discussed above, due to concerns related to the nonbiodegradability of these synthetic polymer coatings, the intention of the present study was to make use of one natural polymer and to study its activity on the release behavior of nanonutrients, upon hydrogel formation with divalent cations. Since the ability of alginic acid to form an SAH and thereby to condition the soil when used in fertilizers has been immensely studied,[11,12] the focus of this study was to monitor how metal oxide nanoparticles attached to the hydrogel matrix and cross-linked metal cations would be released and absorbed when they are complexed with alginic acid. For this, a low-cost nanonutrient particle-based nanofertilizer, where metal oxide nanoparticles act as the nanonutrient particles linked to alginic acid, was synthesized so that the complex can act as a dual-functional fertilizer, which can improve the soil structure by retaining water and deliver micronutrients at the same time. In forming this micronutrient nanofertilizer, as the initial test elements to be incorporated to alginic acid, Zn and Cu were used in their metal oxide forms since previous studies indicate that these metal oxides provide positive effects on plant growth including nourishment of young plants and seedlings, affecting flowering period and enhancing the growth and yield of crops. Considering all of these, the dual functionality of the nanofertilizer that was intended to be synthesized can be summarized as follows; $ZnO_{(s)}$ and $CuO_{(s)}$ nanoparticles act as nanonutrients for the nourishment of young plants and seedlings,[13] while the alginate hydrogel acts as a soil conditioner retaining soil moisture and thereby ensuring that plant roots have better access to nutrients. When the nanofertilizer is applied to plants, metal oxide nanoparticles are readily absorbed by plant roots and are translocated to the shoots. With time and when required, the cations, $Zn_{(aq)}^{2+}$ and $Cu_{(aq)}^{2+}$ cross-linking alginate hydrogels, get absorbed by plant roots and then are translocated to various regions of the plant to carry out metabolic reactions.

Although the use of nanomaterials in agriculture has proved to enhance the productivity and efficiency of crops, there are a variety of safety concerns and health hazards associated with them. Continuous overuse of nanoparticles in agriculture could lead to potential human health and environmental concerns including nonbiodegradability, accumulation, environmental toxicology, and mammalian toxicology.[14] Hence, the amounts and techniques used to synthesize and incorporate nanoparticles in agrochemicals have to be precisely controlled and continuously monitored to minimize the potential health hazards associated with the use of nanomaterials in agriculture. Similarly, since incorrect dosage of fertilizer applied to crop plants can lead to accumulation of salt in soil over time and eventually lead to environmental pollution and soil toxicity, the amounts of metal oxide nanoparticles incorporated with the alginate hydrogel in the development of this micronutrient

https://doi.org/10.1021/acsomega.1c03271
ACS Omega 2021, 6, 26262−26272

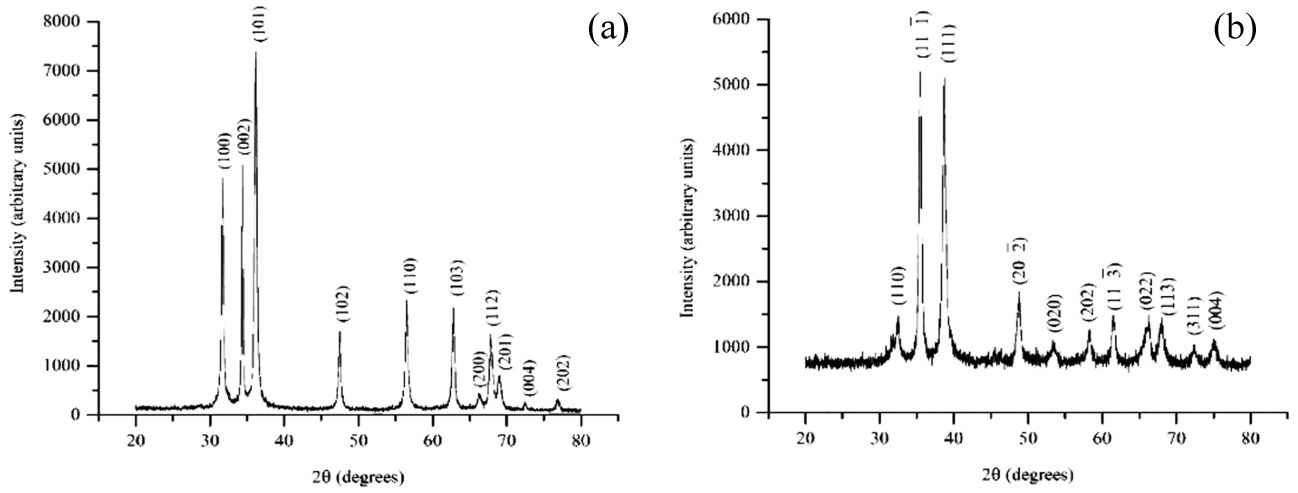

Figure 1. XRD pattern of ZnO nanoparticles (a) with no other peaks except for the characteristic peaks for ZnO. XRD pattern of CuO nanoparticles (b) with the characteristic peaks for CuO. These sets of obtained peaks imply that the synthesized ZnO and CuO nanoparticles were pure and free from impurities.

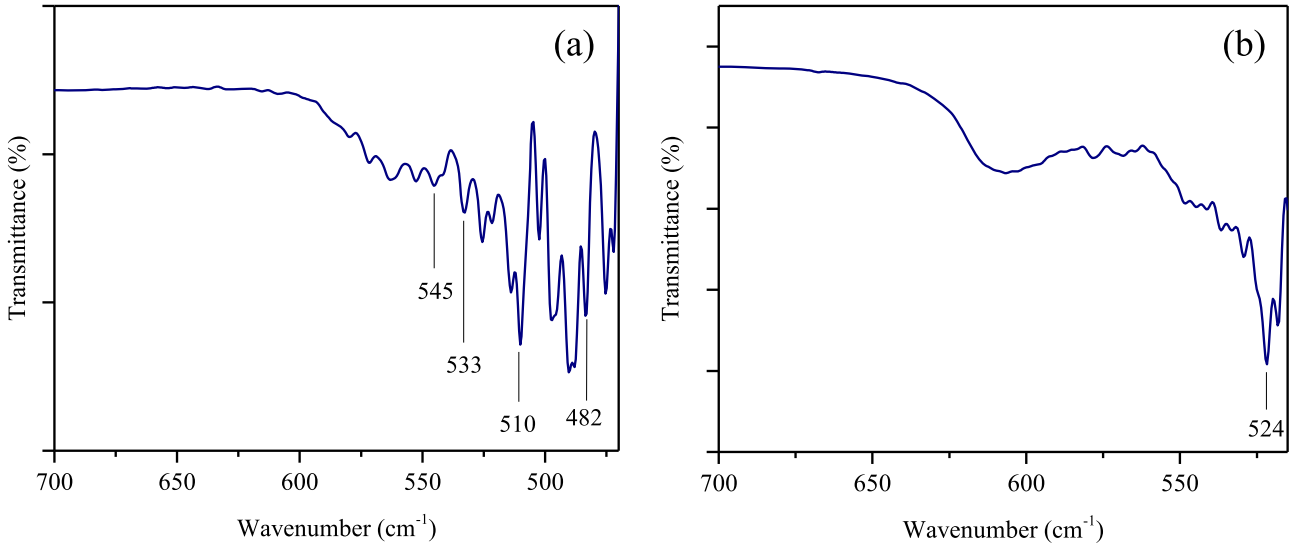

Figure 2. FTIR spectra of ZnO nanoparticles (a) and CuO nanoparticles (b), showing the characteristic peaks for Zn−O and Cu−O stretching modes.

nanofertilizer were precisely controlled to minimize nutrient quantity loss and prevent environmental accumulation.[1]

RESULTS AND DISCUSSION

Although micronutrients are needed in lesser amounts compared to primary and secondary plant nutrients, insufficient levels of these micronutrients could lead to numerous diseases affecting proper vegetation. As discussed above, the main objective of this study was to develop a polymeric fertilizing complex by combining micronutrient metal oxide nanoparticles and a natural polymer and thereby to monitor the absorption and release of micronutrients to plants and the surrounding environments, without the usage of nonbiodegradable compounds. In the formation of the nanofertilizer, Zn and Cu were chosen as the elements to be initially tested to form the complex because of the ease of forming their metal oxide nanoparticles and their important role in plant health. By studying the behavior of this complex in different environments and its uptake by plants, the feasibility of using this polymeric complex as a nanofertilizer was determined.

Characterization of the starting materials and the final polymeric complex revealed that alginic acid has been successfully cross-linked by both $Zn_{(aq)}^{2+}$ and $Cu_{(aq)}^{2+}$ while certain amounts of metal oxide nanoparticles were embedded on the alginate matrix. Experiments conducted on the behavior of the nanofertilizer in soil and water environments and on the uptake by plants showed that there was no hindrance for the release of metal oxide nanoparticles and cations from the alginate matrix and that they would be released into their surrounding under ambient conditions. Hence, these observations confirmed that this nano-ZnO−CuO polymeric material can be developed into a complex in which alginate chains are cross-linked with multiple cationic minerals vital for plant growth and thereby to produce a multifunctional nanofertilizer capable of delivering all micronutrient cations and metal oxide nanoparticles important for healthy growth of plants.

Characterization of Synthesized ZnO and CuO Nanoparticles. X-ray diffraction (XRD) patterns of ZnO and CuO nanoparticles were obtained using a Rigaku Ultima IV X-ray diffractometer with Cu Kα radiation (λ = 0.15418 nm). ZnO nanoparticles were characterized in the diffraction angle range

https://doi.org/10.1021/acsomega.1c03271
ACS Omega 2021, 6, 26262−26272

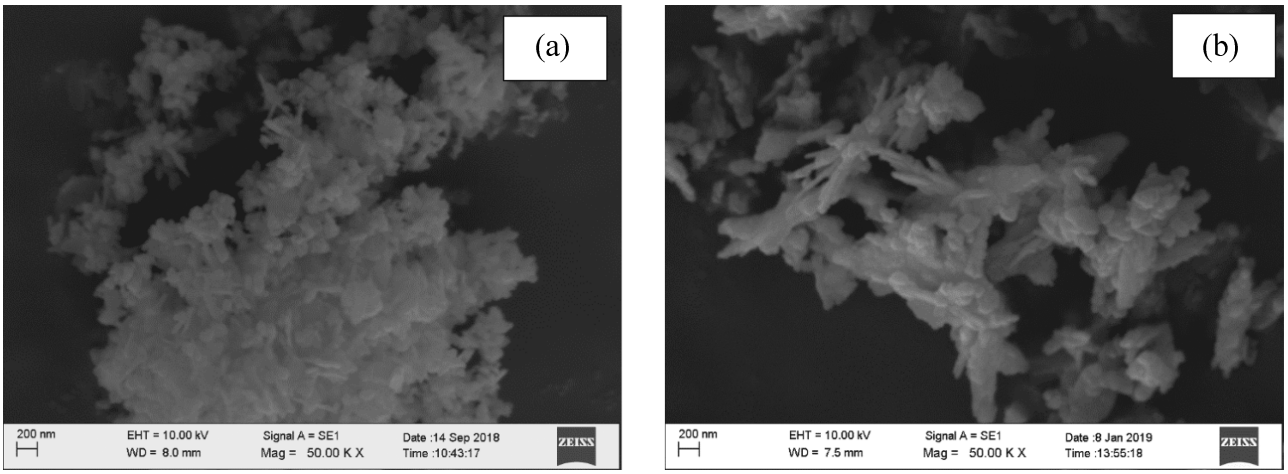

Figure 3. SEM images of spherical-shaped ZnO nanoparticles (a) and elongated platelike CuO nanoparticles (b) showing aggregate nanoparticles.

$20° \leq 2\theta \leq 80°$ (Figure 2a). The sharp peaks obtained at 2θ = 31.74, 34.38, 36.24, 47.55, 56.60, 62.82, 66.59, 67.96, 69.08, 72.61, and 76.86° were assigned to the (1,0,0), (0,0,2), (1,0,1), (1,0,2), (1,1,0), (1,0,3), (2,0,0), (1,1,2), (2,0,1), (0,0,4), and (2,0,2) planes, respectively, and they were in accordance with the literature that have characterized the well-formed structure of ZnO,[15] confirming the purity of the synthesized ZnO nanoparticles.

The XRD pattern of CuO NP was obtained in the diffraction angle range $20° \leq 2\theta \leq 80°$ (Figure 2b). Peaks obtained at 2θ = 32.49, 35.48, 38.68, 48.75, 53.44, 58.23, 61.47, 66.27, 68.09, 72.42, and 74.91° can be assigned to the (1,1,0), (1,1,−1), (1,1,1), (2,0,−2), (0,2,0), (2,0,2), (1,1,−3), (0,2,2), (1,1,3), (3,1,1), and (0,0,4) planes, respectively.[16] The peaks obtained suggested that pure CuO nanoparticles have been formed (Figure 1).

The Fourier transform infrared (FTIR) spectra of the synthesized nanoparticles were obtained using the Thermo Scientific Nicolet iS10 infrared spectrometer by the attenuated total reflection (ATR) technique. Due to the interatomic vibrations of these nanoparticles, metal oxides give significant absorption peaks below 1000 cm^{-1}. Although these nanoparticles were analyzed in the range of 450−4000 cm^{-1}, due to the high intensity in the transmittance peaks below 500 cm^{-1}, peaks at higher wavenumbers were not clearly observed. But since the characteristic vibrations of the stretching frequencies of the metal oxides occurred in lower wavenumbers, purity and the nature of the nanoparticles could be determined.

The significant bands needed to characterize ZnO nanoparticles were present in the range of 450−700 cm^{-1} (Figure 2a). The peak at around 545 cm^{-1} is a characteristic absorption peak for Zn−O.[17] The sharp peak at 510 cm^{-1} corresponds to the vibrational phonon of ZnO.[18] The band at 482 cm^{-1} corresponds to the stretching mode of Zn−O.[19] Furthermore, the band observed at 533 cm^{-1} in the FTIR spectrum of ZnO can be correlated to the transverse optical stretching modes of Zn−O.[20] Hence, the presence of these bands also authenticates the purity and the successful synthesis of ZnO nanoparticles. CuO nanoparticles showed some characteristic peaks in the range 515−650 cm^{-1} (Figure 2b).[21] The tension mode between Cu−O is shown from the band obtained at 522 cm^{-1}.[22] The stretching modes between Cu−O are attributed to the peaks obtained between 522 and 527 cm^{-1},[23] The presence of these bands confirms that CuO nanoparticles have been successfully formed from the synthesis method used.

Morphological characterization of metal oxide nanoparticles using the scanning electron microscope ZEISS EVO|LS15 indicated that the crystallite size of ZnO nanoparticles was between 80 and 100 nm and that of CuO nanoparticles was between 80 and 90 nm (Figure 3).

Characterization of Freeze-Dried Hydrogels. Although the target complex in this research project is nano-ZnO−CuO alginate, nano-ZnO alginate (comprising only ZnO nanoparticles) and nano-CuO alginate (comprising only CuO nanoparticles) were also synthesized to determine the behavior and the distribution of nanoparticles on the alginate matrix. Nano-ZnO alginate appeared in white color, while nano-CuO alginate in brown color and nano-ZnO−CuO showed a combination of white, blue, and light brown colors in the resulting hydrogel, due to the presence of two types of cations and metal oxides (Figure 4).

Figure 4. Synthesized nano-ZnO−CuO alginate showing ZnO NP and CuO NP dispersed in Zn−Cu alginate matrix. This hydrogel showed a combination of properties of both nano-ZnO hydrogel and nano-CuO hydrogel.

The proposed hypothesis for the formation of nano-ZnO−CuO alginate is that, when $HNO_{3(aq)}$ is added to ZnO and CuO nanoparticles, a portion of both types of nanoparticles reacts with $HNO_{3(aq)}$ to form Zn $(NO_3)_{2(aq)}$ and Cu $(NO_3)_{2(aq)}$ while the unreacted nanoparticles remain in the hydrogel as clusters. The formed Zn $(NO_3)_{2(aq)}$ and Cu $(NO_3)_{2(aq)}$ then participate in the formation of the hydrogel. That is, $Zn_{(aq)}^{2+}$ and $Cu_{(aq)}^{2+}$

https://doi.org/10.1021/acsomega.1c03271
ACS Omega 2021, 6, 26262−26272

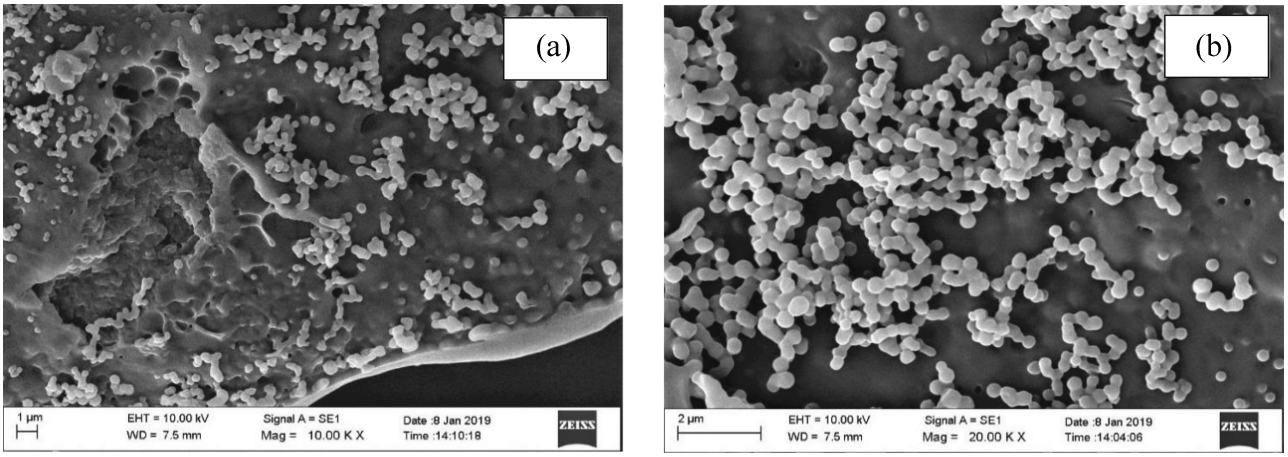

Figure 5. SEM images of nano-ZnO alginate showing clusters of ZnO NP in the alginate matrix (a). Here, it was clearly seen that while certain nanoparticles were dispersed on the alginate matrix, some were embedded in the matrix (b).

replace $Na_{(aq)}^{+}$ in sodium alginate cross-linking alginate chains, resulting in of Zn−Cu alginate. The excess ZnO and CuO nanoparticles then get distributed throughout Zn−Cu−alginate chains, forming the target complex nano-ZnO−CuO alginate.

SEM characterization of nano-ZnO alginate (Figure 5) clearly showed the presence and dispersion of ZnO nanoparticles throughout the matrix. It was also observed that these ZnO nanoparticles are slightly agglomerated and are present on the surface and embedded in the alginate matrix.

SEM analysis of nano-CuO alginate showed the distribution of partially spherical and elongated nanostructures, which could possibly be CuO nanoparticles (Figure 6).

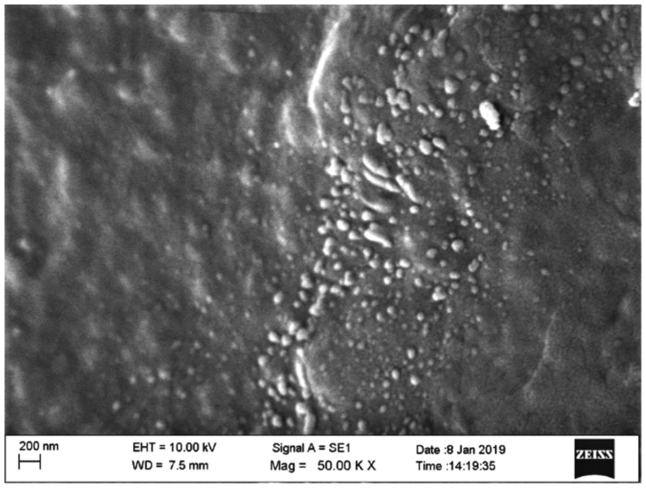

Figure 6. SEM image of nano-CuO alginate showing elongated CuO NP distributed on the CuO alginate matrix.

The flat and circular nanostructures observed in the SEM images of nano-ZnO−CuO alginate could possibly be ZnO nanoparticles while the slightly elongated particles could be CuO nanoparticles (Figure 7). Figure 7b clearly shows that certain foreign particles which are not bound to the matrix are dispersed throughout the matrix. These nanostructures could be suggested to be CuO nanoparticles.

SEM characterization of freeze-dried hydrogels confirmed the dispersion of ZnO and CuO nanoparticles throughout the alginate matrix. It was also observed that some of these nanoparticles are distributed on the superficial layers of the matrix while some nanoparticles were embedded in the matrix.

FTIR characterization of sodium alginate (Figure 8), which is used as the base material for the formation of hydrogels, showed two prominent bands, one broad band and two less intense bands in its spectrum. The intense transmittance band at 3323 cm^{-1} corresponds to the stretching vibration of O−H, while the broad band observed at 2152 cm^{-1} could be attributed to the CO_2 group.[10] The bands observed at 1635 and 1410 cm^{-1} were attributed to the asymmetric and symmetric stretching vibrations of the carboxylate groups, respectively and the less intense band at 1036 cm^{-1} corresponds to the stretching vibration of the C−O−C bond.[24]

The FTIR spectrum of nano-ZnO−CuO alginate (Figure 9) showed a combination of bands in the spectra of ZnO NP, CuO NP, and sodium alginate. The peak observed at 3323 cm^{-1} in the sodium alginate spectrum has shifted to 3261 cm^{-1} in nano-ZnO−CuO alginate. This peak broadening is a result of the intermolecular hydrogen bonding between ZnO NP and CuO NP with the alginate matrix.[25] Cross-linking of alginate chains by $Zn_{(aq)}^{2+}$ and $Cu_{(aq)}^{2+}$ ions has caused a decrease in wavenumber of the carboxylate peak observed at 1635 to 1600 cm^{-1} and 1410 to 1403 cm^{-1}.[26] Since COO^{-} groups in the alginate chains participate in the bonding of these divalent cations, when alginate chains are cross-linked by these it causes more stretching of the COO^{-} groups. As a result of the increase in the bond length between C−O, the peak shifts to a lower wavenumber. The shifting of the asymmetric stretching vibration of the COO^{-} peak can also be explained using the change in the charge density of the cross-linking ion. Here a shifting of the band to a lower wavenumber should be expected because the replacement of Na^{+} in the alginate matrix by Zn^{2+} and Cu^{2+} causes a change in the charge density, atomic weight, and ionic radius.[27] Apart from these significant peak shifts, the other band observed at 1315 cm^{-1} could be attributed to the asymmetrical stretching of C−O group, 1087 and 1028 cm^{-1} bands to the other stretching vibrations associated with C−O group and 819 cm^{-1} to the C−H group vibration of the pyranose group in the alginate ring.[10] These FTIR observations suggest that the polymeric alginate chains have been successfully cross-linked by $Zn_{(aq)}^{2+}$ and $Cu_{(aq)}^{2+}$ with ZnO and CuO NP being held on the matrix by hydrogen bonding. Furthermore, the presence of characteristic stretching vibrations related to Zn−O

https://doi.org/10.1021/acsomega.1c03271
ACS Omega 2021, 6, 26262−26272

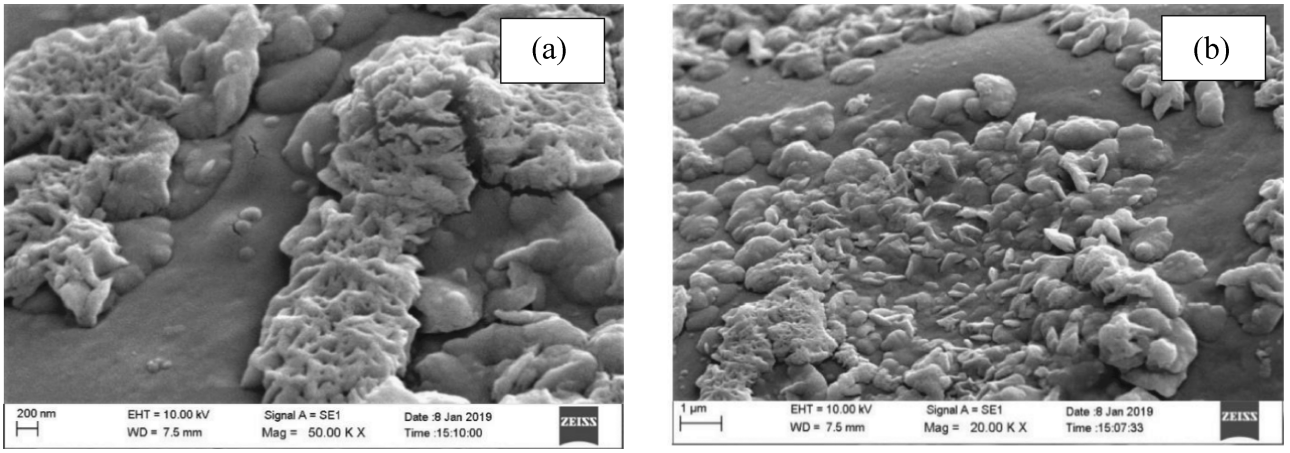

Figure 7. SEM images of nano-ZnO−CuO alginate showing ZnO and CuO NP distributed in the alginate matrix. The flat and circular nanostructures could possibly be ZnO NP (a), while the slightly elongated ones could be CuO NP (b).

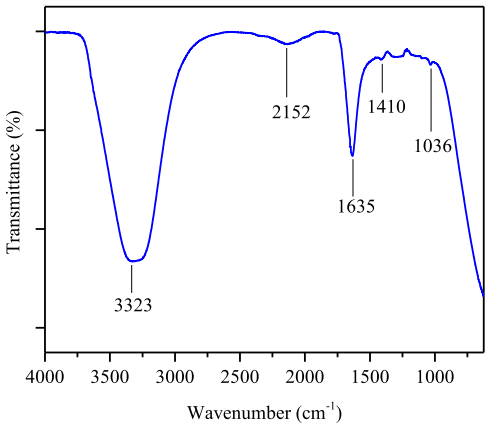

Figure 8. FTIR spectrum of sodium alginate, the base material for the formation of alginate hydrogels. This spectrum showed two prominent bands and two minor bands related to the stretching vibrations of hydroxyl and carboxylate groups in sodium alginate.

and Cu−O vibrations at lower wavenumbers confirmed the presence of ZnO and CuO NP in the combined hydrogel.

Based on these characterizations of nano-ZnO−CuO through SEM and FTIR analyses, it can be suggested that metal oxide nanoparticles embedded in the alginate matrix are chemically bonded while those nanoparticles present on the superficial layers of the matrix are held by weak interactions. Hence, its structure can be possibly determined to be as follows (Figure 10). In its powdered form, ZnO and CuO nanoparticles are embedded as nanonutrients on a hydrogel matrix formed by Zn(II) and Cu(II) cross-linked alginate. This kind of arrangement allows the movement of nanonutrients into its surrounding in moist conditions, followed by the release of Zn(II) and Cu(II) from the hydrogel.

Experiments Done to Study the Behavior of the Nanofertilizer. The initial concentration of Zn and Cu in the nanofertilizer was determined by the atomic absorption spectrophotometer. The concentration of Zn in the nanofertilizing complex was obtained to be 107.62 ± 0.629 ppm and that of Cu was 180.54 ± 1.959 ppm. These obtained concentrations of the metals comprise both the free nanoparticles dispersed throughout the hydrogel and the $Zn_{(aq)}^{2+}$ and $Cu_{(aq)}^{2+}$ cross-linking zinc−copper alginate hydrogel.

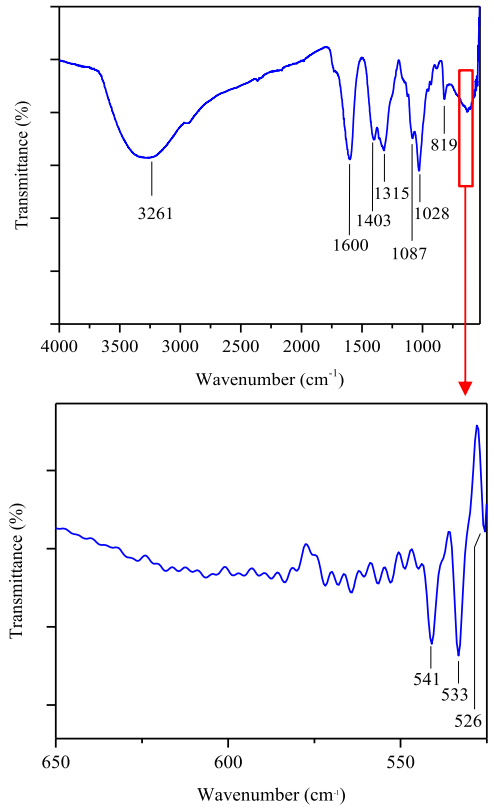

Figure 9. FTIR spectrum of nano-ZnO−CuO alginate showing a combination of bands observed in the IR spectra of sodium alginate, ZnO NP, and CuO NP.

After synthesizing the nanofertilizer and determining its concentration, three experiments were carried out to study the behavior of the nanofertilizer.

(I) Study of the release of the nanofertilizer in water
(II) Study of the release of the nanofertilizer in soil
(III) Study of the uptake of Zn and Cu in the nanofertilizer by tomato leaves

In the experiment to investigate the release behavior of Zn and Cu (present in the nanofertilizer) in water, the tea bag method was used. Here, samples of equal volume were taken out at different time intervals for a period of 240 h and were analyzed for the concentration of Zn and Cu by FAAS (Figure 11). Each

https://doi.org/10.1021/acsomega.1c03271
ACS Omega 2021, 6, 26262−26272

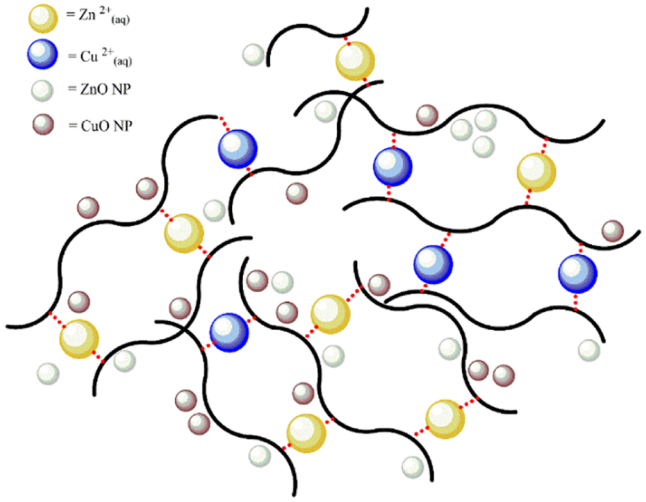

Figure 10. Proposed arrangement for nano-ZnO−CuO hydrogel showing alginic acid chains cross-linked by $Zn_{(aq)}^{2+}$ and $Cu_{(aq)}^{2+}$ with ZnO NP and CuO NP dispersed throughout the cross-linked chains.

time a sample was taken out, deionized water of the same volume was added to the beaker, to keep the volume constant.

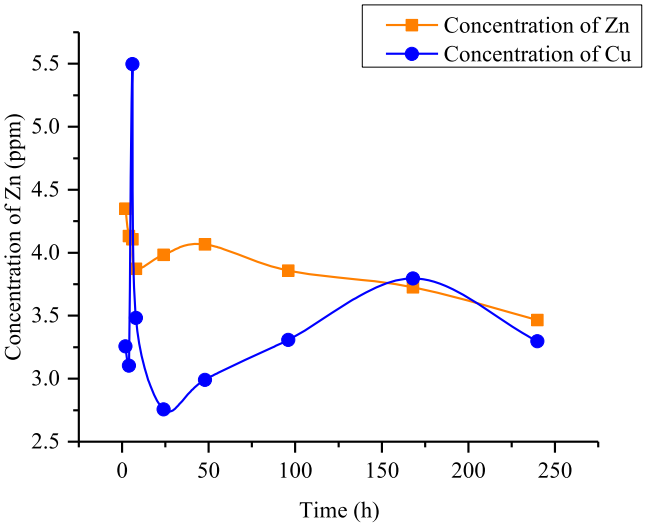

Figure 11. Graph depicting the pattern of release of the nanofertilizer in water that shows the variation of Zn and Cu concentration in water in a period of 240 h.

When considering the release property of Zn and Cu in water, it was observed that high amounts of metals were released within the first 8 h of adding the nanofertilizer to water. This observation could be explained by considering the presence of metal oxide nanoparticles held by weak interactions on the Zn−Cu alginate matrix. As seen on SEM images, excess metal oxide nanoparticles are evenly dispersed throughout the hydrogel on the superficial and deeper layers of the metal alginate matrix. Hence, it can be suggested that, when the nanofertilizer is added to water, since metal oxide nanoparticles on superficial layers of the alginate matrix are held by weak interactions, they get released into the medium first.

After a rapid decrement in their concentrations after 8 h, between 24 and 48 h, there is a slight increment in concentrations of both metals in water, again followed by a decrement. With time, the freeze-dried nanofertilizer starts to swell, and hence, metal oxide nanoparticles present in the deeper layers of the alginate hydrogel could be released into the medium. This could be a reason for the increase in the concentration of metal ions after 24 h.

Figure 12 shows the percentage release of Zn and Cu in water with time, compared to the total amount of these metals released

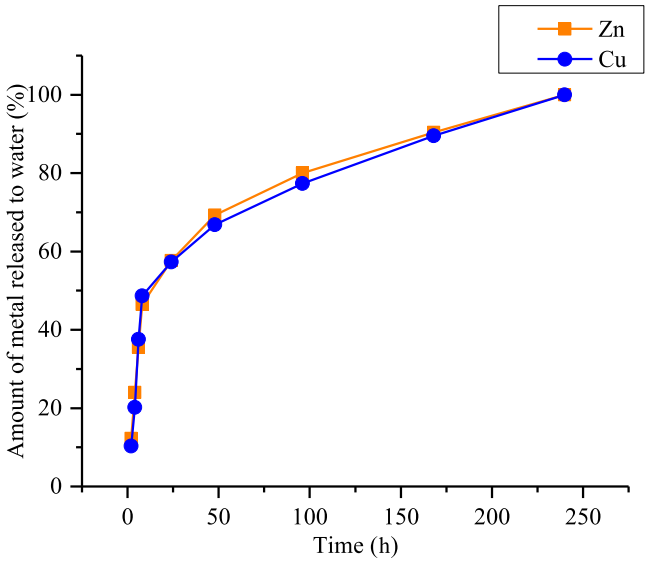

Figure 12. Percentage release of the nanofertilizer with time in water, compared to the total amount released within the experimentation period.

to water within the experimental period. These observations reveal that more than 50% of total Zn and Cu released throughout the experimentation period occurred within the first 24 h. With time, it was seen that the rate of release of Zn and Cu has continued to increase at a slower rate. The reason for this type of change in the metal release rate could be due to the above-discussed reason since the presence of more metal oxide nanoparticles on the surface of the alginate matrix causes them to be released at a faster rate than the embedded metal oxides and the cations linking the alginate chains.

The same explanation could be used to explain the release behavior of the metals in soil during the 30-day period, in which the initial high concentrations of Zn and Cu could be due to the metal oxide nanoparticles embedded on the surface of the matrix while the subsequent reduction in concentration could be because the release of cations cross-linking alginate chains takes some time (Figure 13). Although the initial concentration of Cu in the nanofertilizer is higher than that of Zn, the amount of Cu released in soil is lower than the amount of Zn released. The high affinity of copper to organic matter and soil colloids due to its high sorption capacity, the decrease in copper mobilization in soils by heterotrophic bacteria, and the complexing of copper with other minerals in soil could be the major reasons for the reduction in Cu concentration in soil than that of Zn.[2829]

The percentage release of Zn and Cu in soil showed a gradual increment (Figure 14). It was observed that more than 50% of the total Zn and Cu released throughout the experimentation period, was released within the first 10 days of adding the nanofertilizer to soil. The rate of release of metals has gradually reduced with time.

Study of the Uptake of Zn and Cu in the Nanofertilizer by Tomato Plants. This experiment was carried out by adding

https://doi.org/10.1021/acsomega.1c03271
ACS Omega 2021, 6, 26262−26272

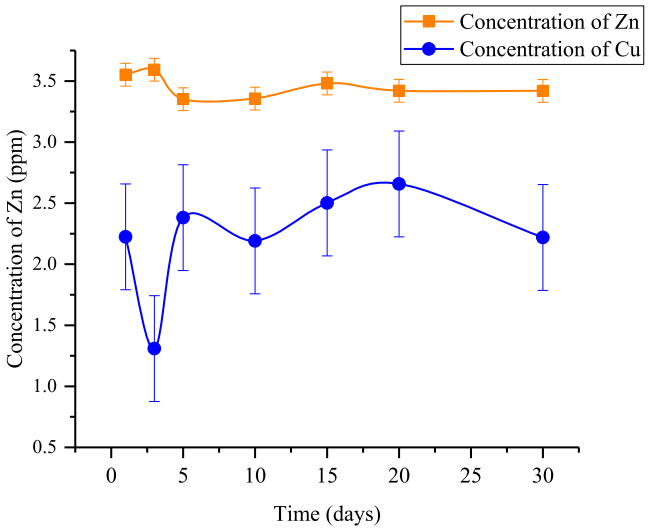

Figure 13. Release behavior of the nanofertilizer in soil showing the variation in the concentrations of Zn and Cu in soil for a period of 30 days.

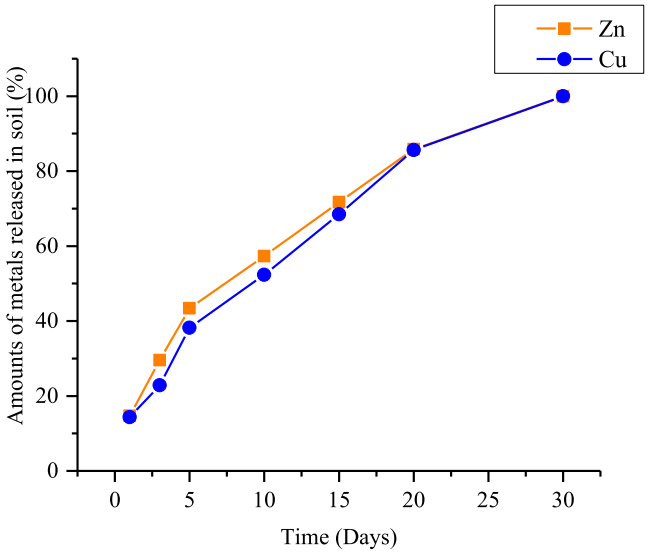

Figure 14. Percentage release of the nanofertilizer with time in soil, compared to the total amount released within the experimentation period.

different combinations of the nanofertilizer and a natural fertilizer to four tomato beds. These tomato beds were cultivated in sandy loam soil with the soil pH adjusted to 5.5−7.5. The natural fertilizer was formed by mixing certain kitchen wastes that provide basic nutrients including N, P, K, and Ca to plants. The kitchen wastes used here were eggshells, fish bones, and used coffee grounds. The purpose of adding this natural fertilizer to tomato beds was to make sure that the uptake of the metals in the nanofertilizer was still occurring even in the presence of another compound capable of providing N, P, K nutrients to plants. This was also done to determine if any negative impacts were caused when the fertilizing effects of the nanofertilizer combined with the composting effects of the natural fertilizer added. Henceforth for the first bed ("0.1") 100 mg and for the second bed ("0.2") 200 mg of the nanofertilizer was added. For the third bed ("0.2 + C"), 200 mg of the nanofertilizer was added along with a predetermined amount of the natural fertilizer and as the control, for the fourth bed ("C") only the natural fertilizer was added.

The initial concentrations of Zn and Cu in soil, determined using ethylenediaminetetraacetic acid (EDTA) extraction, were as follows (Table 1).

Table 1. Initial Concentrations of Zn and Cu in Soil

metal ion	concentration (ppm)
Zn(II)	9.2908
Cu(II)	1.3342

Prior to the addition of the nanofertilizer to the tomato beds, the initial concentrations of Zn and Cu in tomato leaves were measured in two stages of the growth of the plants; 30 days and 70 days after planting the seeds. The obtained concentrations of Zn(II) and Cu(II) in the initial analysis of tomato leaves during the two stages can be depicted as follows (Table 2).

Table 2. Initial Concentrations of Zn and Cu in Tomato Leaves

metal ion	concentration in growing stage/ppm (30 days after planting the seeds)	concentration in mature stage/ppm (70 days after planting the seeds)
Zn(II)	6.0351	not detected by FAAS
Cu(II)	6.1305	0.1339

The reasons for the reduction in metal concentration as the plant matures could be the dilution of these metals in plant leaves as plant growth occurs and these nutrients being used in many processes such as carbohydrate metabolism, auxin synthesis, protein synthesis, mitochondrial respiration, cell wall metabolism and regulation of gene expression.[30] These processes occur in mature plant stage as well, but activities such as protein and carbohydrate synthesis and hormone production are vital and crucial during growing stages.

When determining the uptake of Zn and Cu by tomato leaves, it was observed that Zn concentrations in all four beds and Cu concentration in the first bed were undetected by FAAS. This could be due to the concentration of Zn and Cu in those beds being lower than the limit of detection (LOD) of these metals for FAAS (LOD of Zn for FAAS-0.01316 ppm, LOD of Cu for FAAS-0.06475 ppm) (Figure 15).

When the 0.2 series is considered, it could be seen that high amounts of Cu have been absorbed by tomato roots and then transported to tomato leaves. In contrast, the uptake of Cu in the 0.2 + C series shows a more gradual and incremental pattern within the time frame experimented. The reason for this pattern can be attributed to the addition of the natural fertilizer along with the nanofertilizer to the tomato bed. This natural fertilizer contains organic matter, and as discussed earlier, Cu-containing CuO nanoparticles have a high affinity to organic matter due to their high sorption capacities.[28] Hence, we can assume that although CuO NPs present in the superficial layers of the alginate matrix are released to the soil, they get adsorbed onto the organic matter and minerals present in the soil. Hence, the increase in the Cu content in leaves is lesser than that in the 0.2 series. Although there are smaller increments and decrements in the Cu concentration in leaves till the 20th day, the overall change is almost constant. This can be due to the release and the absorption of the nanoparticles embedded in the matrix due to swelling of the freeze-dried alginate hydrogel. Hence, during this

https://doi.org/10.1021/acsomega.1c03271
ACS Omega 2021, 6, 26262−26272

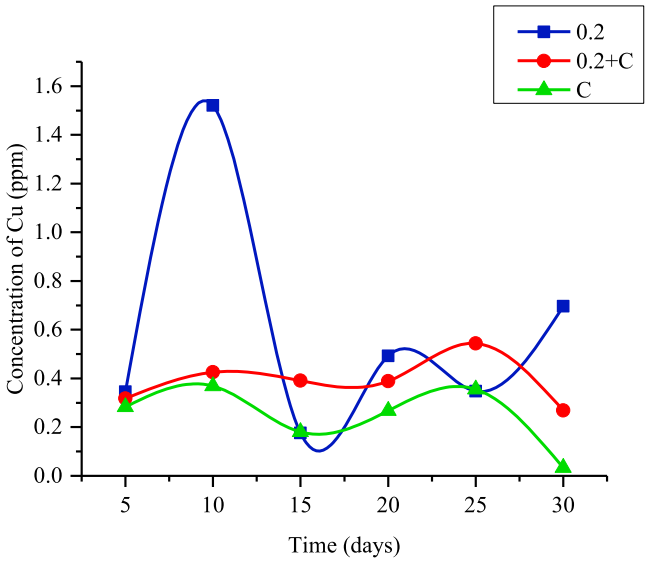

Figure 15. Change in the concentration of Cu in tomato leaves during the 30-day experimentation period. The concentration of Cu in the 0.1 series (to which only 100 mg of the nanofertilizer was added) was not detected by FAAS.

period, this series shows a slow-releasing behavior of Cu into its surrounding environment. The increase in CuO in soil causes a decrease in soil pH, which results in the desorption of adsorbed Cu in organic matter to the soil.[28] Also, the release of $Cu_{(aq)}^{2+}$ ions cross-linking the alginate chains can take place by this time. All of these reasons can increase the amount of Cu in the soil, and eventually this Cu is taken up into the plant system. By day 30, a gradual decrement in the Cu concentration in plant leaves is observed. This type of slow-releasing and slow-absorbing behavior of micronutrients by plants is beneficial for plant growth since absorption of large amounts of micronutrients to plants at once can cause detrimental effects to plants.

The reasons for the reduction in zinc content can be attributed to high levels of phosphorus in soil, which reduces the transmission of zinc from plant roots to shoots or even inhibit the absorption of zinc by plant roots, the "dilution effect" that causes the decrease in zinc concentration in plant parts as growth progresses and the antagonistic relationship between Zn and Cu during xylem loading and unloading.[31]

Post-experimentation Determination of Soil Conditions. The average concentrations of Zn and Cu in soil were determined 60 days after the 30-day-leaf analysis experiment to see whether Zn and Cu have got accumulated in soil. The amounts of Zn and Cu in soil after the experimentation period were well below their maximum permissible levels concluding that there has not been any accumulation of Zn and Cu in soil (Table 3).

Table 3. Zn and Cu Concentrations in Tomato Beds after the Experimentation Period

	concentration in soil in each tomato bed (ppm)				
metal	0.1	0.2	0.2 + C	C	maximum permissible level by WHO (2008)[32] (ppm)
Zn	1.6957	2.6450	2.9884	2.2887	50
Cu	2.1340	2.4045	2.2755	6.6974	30

After the experimentation period, i.e., after 30 days, the soil pH values were measured again. The obtained values are as follows (Table 4).

Table 4. pH Values of Tomato Beds after the Experimentation Period

bed number	tomato bed	pH
1	0.1	7.13
2	0.2	7.28
3	0.2 + C	7.49
4	C	7.47

The third bed, into which both the nanofertilizer and the compost were added, showed the highest pH value after the experimentation period due to the presence of the highest amount of organic matter out of the four beds concerned.

CONCLUSIONS

The aim of this study was to synthesize a plant and soil conditioning micronutrient nanofertilizer by incorporating metal oxide nanoparticles to the biopolymer alginic acid, to monitor the release and absorption behavior of micronutrient metal oxides and cations incorporated with the alginate hydrogel. Synthesis of the micronutrient nanofertilizer was achieved by the formation of Zn−Cu alginate hydrogel, through which ZnO and CuO nanoparticles were dispersed. The synthesis of nanoparticles was done via chemical methods, and their characterization was done by XRD, FTIR, and SEM analyses. The synthesized nanofertilizer, nano-ZnO−CuO alginate, was characterized by FTIR spectroscopy and SEM analysis. FTIR analysis of the synthesized nano-ZnO−CuO alginate hydrogel confirmed the presence of ZnO and CuO nanoparticles and their possible bond formation with the hydrogel. Shifting of wavenumber of the carboxylate peak in nano-ZnO−CuO alginate to lower values confirmed the cross-linking of alginate chains by both $Zn_{(aq)}^{2+}$ and $Cu_{(aq)}^{2+}$. SEM analysis showed the dispersion of metal oxide nanoparticles throughout the alginate matrix, with some being loosely held on the matrix and others embedded in the alginate polymer.

The release ability of micronutrients contained in the nanofertilizer was studied in controlled water and soil environments. Its release behavior suggested that the loosely held metal oxide nanoparticles in the hydrogel get released first followed by the possible release of $Zn_{(aq)}^{2+}$ and $Cu_{(aq)}^{2+}$, cross-linking the polymer chains, to the surrounding environment. The synthesized nanofertilizer was applied to tomato beds and the uptake of Zn and Cu by plant leaves was studied for a period of 30 days. The results suggested that a reduced uptake of Cu has occurred but the amounts of Zn in the leaves were undetected by FAAS. This could possibly be due to Zn uptake being inhibited by soil phosphorus or the antagonistic nature in the uptake of Zn and Cu. The results obtained from these experiments confirmed that although the metal oxide nanoparticles were incorporated onto the alginate matrix, these have the ability to be released into the surrounding environment under ambient conditions and also could be easily absorbed by the plant root systems, even in the presence of an NPK fertilizer. Hence, it was noted that this polymeric fertilizing complex introduced in this study has the potential to be further developed into a multifunctional micronutrient nanofertilizer, which has the ability to provide all types of micronutrients to crop plants, while nourishing the soil to an organic state.

https://doi.org/10.1021/acsomega.1c03271
ACS Omega 2021, 6, 26262−26272

METHODS

Synthesis of ZnO and CuO Nanoparticles. An aqueous solution of 0.1 mol dm^{-3} $Zn(NO_3)_2.6H_2O$ $ZnO_{(s)}$ was mixed with a 0.8 M NaOH aqueous solution under high-speed stirring for 2 h, on a magnetic stirrer, to synthesize ZnO nanoparticles. After allowing the solution to settle overnight, the supernatant was separated and the formed precipitate was cleaned with water and ethanol. Finally, the precipitated ZnO nanoparticles were dried in air atmosphere at 60 °C.[33] During drying, $Zn(OH)_{2(s)}$ was completely converted to $ZnO_{(s)}$ nanoparticles. CuO nanoparticles were synthesized using the chemical precipitation method. For this, the 1.0 M NaOH solution was added dropwise into the $CuCl_2.2H_2O_{(aq)}$ solution under constant stirring. The formed brown precipitate $Cu(OH)_{2(s)}$ was washed with distilled water and then centrifuged to remove the native impurities in the product. The $Cu(OH)_{2(s)}$ precipitate was then calcined at 350 °C for 2 h in air, during which $Cu(OH)_{2(s)}$ completely turned into $CuO_{(s)}$ nanoparticles.[34]

Synthesis of Nano-ZnO Alginate and Nano-CuO Alginate. In the formation of nano-ZnO alginate, exactly 0.08138 g of ZnO nanoparticles (0.001 mol) was added to 0.129 cm^3 of $HNO_{3(aq)}$ solution. Then, this solution was made to a total volume of 50 cm^3 by adding distilled water. The resulting solution was constantly stirred at a high speed using a magnetic stirrer for 1 h. Then, the $Zn(NO_3)_{2(aq)}$ solution consisting of excess nanoparticles was transferred to a Petri dish. Exactly 25 cm^3 of 2% sodium alginate aqueous solution was added into the solution in the Petri dish without any stirring. Upon the addition of sodium alginate solution, white-colored zinc alginate hydrogel formation was observed.

When forming nano-CuO alginate, exactly 0.07955 g of CuO nanoparticles (0.001 mol) was added to 0.129 cm^3 of $HNO_{3(aq)}$ solution in a volumetric flask. Then, this was made to a total volume of 50 cm^3 by adding distilled water. The resulting solution was constantly stirred at a high speed using a magnetic stirrer for 1 h. This $Cu(NO_3)_{2(aq)}$ solution consisting of excess nanoparticles was transferred to a Petri dish. Exactly 25 cm^3 of 2% sodium alginate aqueous solution was added to the solution in the Petri dish without any stirring. Upon the addition of sodium alginate solution, dark brown-colored copper alginate hydrogel formation was observed.

Synthesis of Nano-ZnO−CuO Alginate. The method of synthesizing nano-ZnO−CuO alginate was quite straightforward. Equimolar amounts of ZnO and CuO nanoparticles in excess were then reacted with an aqueous solution of HNO_3. Distilled water was added to this mixture to make the final volume 50 cm^3. This solution was then transferred to a Petri dish, and exactly 25 cm^3 of 2% sodium alginate solution was added to the above solution. Upon the addition of sodium alginate, dark blue color hydrogel formation was observed, indicating the formation of nano-ZnO−CuO alginate composite. This hydrogel was freeze-dried and characterized by FTIR and SEM techniques.

Experiments Done to Test the Behavior of the Nanofertilizer. *Release Behavior of the Nanofertilizer in Water and Soil.* These experiments were carried out using the tea bag method, in which the nanofertilizer put into a tea bag was placed in water (when studying the release in water) and dry soil (when studying the release in soil). The experiment carried out to study the release in water was done for 240 h. At 2, 4, 6, 8, 24, 48, 96, 168, and 240 h of adding the nanofertilizer to water, samples were pipetted out and analyzed using flame atomic absorption spectrometry to determine the release of Zn and Cu in water. To keep the volume constant throughout the experiment, each time a sample was pipetted out, an equal volume of deionized water was added back to the beaker.

The experiment to study the release behavior of the nanofertilizer in soil was carried out for 30 days, and each experiment was duplicated. A certain amount of tap water was added to the beaker containing dry soil to create an ideal soil environment. At 1, 3, 5, 10, 15, 20, and 30 days, soil samples were taken out, extracted using 0.04 M EDTA, and finally analyzed by flame atomic absorption spectrometry. During this study, the total mass was kept constant by adding a soil sample of same weight back to the beaker, and every time a sample was taken out.[35]

Study of the Uptake of the Nanofertilizer by Tomato Plants. For this experiment, four tomato beds were prepared with sandy loam soil with five tomato plants in each bed. To the first and second beds, exactly 100 and 200 mg of the nanofertilizer were added, respectively. To the third bed, 200 mg of the nanofertilizer was added along with a natural fertilizer, in the form of a compost, made using crushed eggshells, fish bones, and used coffee grounds that mainly provides N, P, K, Ca, Na, and Mg to plants. The purpose of adding this compost was to determine whether the uptake of the nanofertilizer by plants was still occurring in the presence of another fertilizer that provides N, P, and K nutrients to plants. As the control, to the fourth bed, only the natural fertilizer was added. After applying the nanofertilizer, tomato leaves were collected every fifth day for a period of 30 days.

These leaves were oven-dried for 1 h followed by heating in a muffle furnace at 450 °C for 8 h. The dry ash obtained was then digested using 25% (v/v) $HNO_{3(aq)}$.[36] Finally, the obtained solution was filtered using a syringe filter analyzed for Zn and Cu by flame atomic absorption spectrophotometry.

AUTHOR INFORMATION

Corresponding Author

Pahan I. Godakumbura − *Department of Chemistry, Faculty of Applied Sciences, University of Sri Jayewardenepura, Nugegoda 10250, Sri Lanka;* orcid.org/0000-0002-7742-3859; Email: pahanig@sjp.ac.lk

Author

S. Amanda Ekanayake − *Department of Chemistry, Faculty of Applied Sciences, University of Sri Jayewardenepura, Nugegoda 10250, Sri Lanka*

Complete contact information is available at: https://pubs.acs.org/10.1021/acsomega.1c03271

Notes

The authors declare no competing financial interest.

ACKNOWLEDGMENTS

The authors thank the Department of Chemistry in the University of Sri Jayewardenepura for funding and providing the necessary facilities to conduct this research study, the Instrument Center in the Faculty of Applied Sciences in the University of Sri Jayewardenepura, and the SEM analysis center in the University of Peradeniya for their support with the instrumental operation, analysis, and interpretation of data. They also acknowledge Prabhath Jayarathne for designing the artwork related to this manuscript.

https://doi.org/10.1021/acsomega.1c03271
ACS Omega 2021, 6, 26262−26272

REFERENCES

(1) Mikula, K.; Izydorczyk, G.; Skrzypczak, D.; Mironiuk, M.; Moustakas, K.; Witek-Krowiak, A.; Chojnacka, K. Controlled release micronutrient fertilizers for precision agriculture−A review. *Sci. Total Environ.* **2020**, *712*, No. 136365.

(2) Al-Mamun, M. R.; Hasan, M. R.; Ahommed, M. S.; Bacchu, M. S.; Ali, M. R.; Khan, M. Z. H. Nanofertilizers towards sustainable agriculture and environment. *Environ. Technol. Innovation* **2021**, *23*, No. 101658.

(3) Singh, M. D.; Gautam, C.; Patidar, O.; Meena, H. Nano fertilizers is a new way to increase nutrients use efficiency in crop production. *Int. J. Agric. Sci.*. **2017**, *9*, 3831−3833.

(4) Veronica, N.; Guru, T.; Thatikunta, R.; Reddy, S. N. Role of Nano Fertilizers in Agricultural Farming. *Int. J. Environ. Sci. Technol* **2015**, *1*, 1−3.

(5) Ramli, R. A. Slow release fertilizer hydrogels: a review. *Polym. Chem.* **2019**, *10*, 6073−6090.

(6) Shen, Y.; Wang, H.; Li, W.; Liu, Z.; Liu, Y.; Wei, H.; Li, J. Synthesis and characterization of double-network hydrogels based on sodium alginate and halloysite for slow release fertilizers. *Int. J. Biol. Macromol.* **2020**, *164*, 557−565.

(7) Di Martino, A.; Khan, Y. A.; Durpekova, S.; Sedlarik, V.; Elich, O.; Cechmankova, J. Ecofriendly renewable hydrogels based on whey protein and for slow release of fertilizers and soil conditioning. *J. Cleaner Prod.* **2021**, *285*, No. 124848.

(8) Thakur, S.; Arotiba, O. A. Synthesis, swelling and adsorption studies of a pH-responsive sodium alginate−poly(acrylic acid) superabsorbent hydrogel. *Polym. Bull.* **2018**, *75*, 4587−4606.

(9) Zhang, M.; Zhao, X. Alginate hydrogel dressings for advanced wound management. *Int. J. Biol. Macromol.* **2020**, *162*, 1414−1428.

(10) Lopes, S.; Bueno, L.; AGUIAR, F. D.; Finkler, C. Preparation and characterization of alginate and gelatin microcapsules containing *Lactobacillus rhamnosus*. *An. Acad. Bras. Cienc.* **2017**, *89*, 1601−1613.

(11) Rashidzadeh, A.; Olad, A. Slow-released NPK fertilizer encapsulated by NaAlg-g-poly (AA-co-AAm)/MMT superabsorbent nanocomposite. *Carbohydr. Polym.* **2014**, *114*, 269−278.

(12) Rashidzadeh, A.; Olad, A.; Salari, D.; Reyhanitabar, A. On the preparation and swelling properties of hydrogel nanocomposite based on sodium alginate-g-poly (acrylic acid-co-acrylamide)/clinoptilolite and its application as slow release fertilizer. *J. Polym. Res.* **2014**, *21*, No. 344.

(13) Sabir, S.; Arshad, M.; Chaudhari, S. K. Zinc Oxide Nanoparticles for Revolutionizing Agriculture: Synthesis and Applications. *Sci. World J.* **2014**, *2014*, 1−8.

(14) Singh, R. P. Application of Nanomaterials Toward Development of Nanobiosensors and their Utility in Agriculture. In *Nanotechnology*, Springer, 2017; pp 293−303.

(15) Madhumitha, G.; Fowsiya, J.; Gupta, N.; Kumar, A.; Singh, M. Green synthesis, characterization and antifungal and photocatalytic activity of Pithecellobium dulce peel−mediated ZnO nanoparticles. *J. Phys. Chem. Solids* **2019**, *127*, 43−51.

(16) Apriandanu, D. O. B.; Yulizar, Y. Tinospora crispa leaves extract for the simple preparation method of CuO nanoparticles and its characterization. *Nano-Struct. Nano-Objects* **2019**, *20*, No. 100401.

(17) Khan, M.; Naqvi, A. H.; Ahmad, M. Comparative study of the cytotoxic and genotoxic potentials of zinc oxide and titanium dioxide nanoparticles. *Toxicol. Rep.* **2015**, *2*, 765−774.

(18) Getie, S.; Belay, A.; Chandra Reddy, A.; Belay, Z. Synthesis and Characterizations of Zinc Oxide Nanoparticles for Antibacterial Applications. *J. Nanomed. Nanotechnol.* **2017**, *8*, No. 4.

(19) Basha, S. K.; Lakshmi, K. V.; Kumari, V. S. Ammonia sensor and antibacterial activities of green zinc oxide nanoparticles. *Sens., Bio Sens. Res.* **2016**, *10*, 34−40.

(20) Lefatshe, K.; Muiva, C. M.; Kebaabetswe, L. P. Extraction of nanocellulose and in-situ casting of ZnO/cellulose nanocomposite with enhanced photocatalytic and antibacterial activity. *Carbohydr. Polym.* **2017**, *164*, 301−308.

(21) Prakash, V.; Diwan, R. Characterization of synthesized copper oxide nanopowders and their use in nanofluids for enhancement of thermal conductivity. *Indian J. Pure Appl. Phys.* **2015**, *53*, 753−758.

(22) Safaei, M.; Taran, M. Optimized synthesis, characterization, and antibacterial activity of an alginate−cupric oxide bionanocomposite. *J. Appl. Polym. Sci.* **2018**, *135*, No. 45682.

(23) Sackey, J.; Nwanya, A. C.; Bashir, A. K. H.; Matinise, N.; Ngilirabanga, J. B.; Ameh, A. E.; Coetsee, E.; Maaza, M. Electrochemical properties of *Euphorbia pulcherrima* mediated copper oxide nanoparticles. *Mater. Chem. Phys.* **2020**, *244*, No. 122714.

(24) Barreto, M. S. R.; Andrade, C. T.; da Silva, L. C. R. P.; Cabral, L. M.; Flosi Paschoalin, V. M.; Del Aguila, E. M. In vitro physiological and antibacterial characterization of ZnO nanoparticle composites in simulated porcine gastric and enteric fluids. *BMC Vet. Res.* **2017**, *13*, No. 181.

(25) Mohandas, A.; Kumar, P.T.S.; Raja, B.; Lakshmanan, V.; Jayakumar, R. Exploration of alginate hydrogel/nano zinc oxide composite bandages for infected wounds. *Int. J. Nanomed.* **2015**, *10*, 53−66.

(26) Mandal, B.; Alexander, K.; Riga, A. Evaluation of the drug-polymer interaction in calcium alginate beads containing diflunisal. *Pharmazie* **2010**, *65*, 106−109.

(27) Daemi, H.; Barikani, M. Synthesis and characterization of calcium alginate nanoparticles, sodium homopolymannuronate salt and its calcium nanoparticles. *Sci. Iran.* **2012**, *19*, 2023−2028.

(28) Vlček, V.; Pohanka, M. Adsorption of Copper in Soil and its Dependence on Physical and Chemical Properties. *Acta Univ. Agric. Silvic. Mendelianae Brun.* **2018**, *66*, 219−224.

(29) Štyriaková, D.; Štyriaková, I.; Štyriak, I.; Šuba, J.; Danková, Z.; Gešperová, D. Inhibition Effect of Heterotrophic Microorganisms on Cu and Zn Cations Mobilization from Contaminated Soil and Sediment. *Procedia Earth Planet. Sci.* **2015**, *15*, 866−871.

(30) Xiong, T.; Zhang, T.; Dumat, C.; Sobanska, S.; Dappe, V.; Shahid, M.; Xian, Y.; Li, X.; Li, S. Airborne foliar transfer of particular metals in *Lactuca sativa* L.: translocation, phytotoxicity, and bioaccessibility. *Environ. Sci. Pollut. Res.* **2019**, *26*, 20064−20078.

(31) Kutrowska, A.; Małecka, A.; Piechalak, A.; Masiakowski, W.; Hanć, A.; Barałkiewicz, D.; Andrzejewska, B.; Zbierska, J.; Tomaszewska, B. Effects of binary metal combinations on zinc, copper, cadmium and lead uptake and distribution in *Brassica juncea*. *J. Trace Elem. Med. Biol.* **2017**, *44*, 32−39.

(32) Sanusi, K. A.; Hassan, M. S.; Abbas, M. A.; Kura, A. M. Assessment of heavy metals contamination of soil and water around abandoned Pb-Zn mines in Yelu, Alkaleri Local Government Area of Bauchi State, Nigeria. *Int. Res. J. Pub. Environ. Health* **2017**, *4*, 72−77.

(33) Talam, S.; Karumuri, S. R.; Gunnam, N. Synthesis, Characterization, and Spectroscopic Properties of ZnO Nanoparticles. *ISRN Nanotechnol.* **2012**, *2012*, 1−6.

(34) Gopalakrishna, D.; Vijayalakshmi, K.; Ravidhas, C. Effect of annealing on the properties of nanostructured CuO thin films for enhanced ethanol sensitivity. *Ceram. Int.* **2013**, *39*, 7685−7691.

(35) Baki, M.; Abedi-Koupai, J. Preparation and characterization of a superabsorbent slow-release fertilizer with sodium alginate and biochar. *J. Appl. Polym. Sci.* **2018**, *135*, No. 45966.

(36) Karpiuk, U. V.; Al Azzam, K. M.; Abudayeh, Z. H. M.; Kislichenko, V.; Naddaf, A.; Cholak, I.; Yemelianova, O. Qualitative and Quantitative Content Determination of Macro-Minor Elements in *Bryonia alba* L. Roots using Flame Atomic Absorption Spectroscopy Technique. *Adv. Pharm. Bull.* **2016**, *6*, 285−291.

https://doi.org/10.1021/acsomega.1c03271
ACS Omega 2021, 6, 26262−26272